Journal of Magnetics 9(2), 47-51 (2004)

Giant Magnetoimpedance in $Co_{67}Fe_4Mo_{1.5}Si_{16.5}B_{11}$ Metallic Glass Ribbon

M. Kuźmiński[1]*, K. Nesteruk[1], H. K. Lachowicz[1], A. Krzyżewski[1], Seong-Cho Yu[2], Heebok Lee[3] and Cheol Gi Kim[4]

[1]*Institute of Physics, Polish Acad. of Sci., Al. Lotników 32/46, 02-668 Warsaw, Poland*
[2]*Chungbuk National Univ., Physics, Cheongju 361-763, Korea*
[3]*Kongju National University, Dept. of Physics, Kongju 314-701, Korea*
[4]*Chungnam National Univ., Materials Engineering, Daejeon 305-764, Korea*

(Received 20 February 2004)

Giant magneto-impedance (GMI) effect in zero-magnetostrictive Co-based amorphous ribbons samples in their as-quenched and stress-released states as well as with intentionally induced magnetic anisotropy were investigated. Magnetic and impedance properties of the samples exhibiting different anisotropy were compared and the optimum operation conditions for the studied samples from the view-point of their utilization as a sensor element have been determined. A design of a model of magnetic field sensor and characteristics of the constructed prototype are presented.

Key words : Giant magneto-impedance, Co-based amorphous ribbon, magnetic anisotropy, magnetic field sensor

1. Introduction

Huge changes in the impedance of a magnetic electrically conducting element in a form of thin wire, ribbon, film or various composite structures, occurred under applied DC-magnetic field, have been observed at sufficiently high frequencies of an AC-current flowing along this element (see e.g. [1]). The effect, called giant magneto-impedance (GMI), may be utilized in magnetic field sensors [1-3] giving good alternative to sensors operating under other principles. From this point of view, high sensitivity as well as other factors like magneto-impedance hysteresis, stability and cost are important. In the present work, GMI effect is studied in magnetically soft, near-zero-magnetostrictive Co-based amorphous ribbons modified by thermal treatment which leads to changes in magnetic and magneto-impedance characteristics of the ribbon because of alterations in local magnetic anisotropy. The material of the studied ribbon exhibits relatively low Curie temperature, therefore to induce magnetic anisotropy by field annealing is rather a difficult task. However, stress annealing procedure can instead be used to create this anisotropy.

*Corresponding author: Tel: +48-22-8436601-3112, e-mail: kuzmi@ifpan.edu.pl

2. Experimental

Magnetically soft 25 μm thick ribbon of the nominal composition $Co_{67}Fe_4Mo_{1.5}Si_{16.5}B_{11}$, produced by melt-spinning technique, was used as a model material. The samples, 6 cm long and 2.2 mm wide, in its as-quenched state (S1) or after annealing in a protective atmosphere were used in the experiments. Some of them were annealed over 1 hour at 250°C (S2) and 350°C (S3) for stress relaxation, as well as at 350°C under tensile stress of 140 MPa (S4), 280 MPa (S5) and 410 MPa (S6) in order to induce transverse magnetic anisotropy.

Quasi-static magnetization characteristics in an axial magnetic field were measured using hysteresis loop tracer. The auto-balancing bridge with four coaxial leads was used to measure two components of the impedance ($Z = R + jX$) in the frequency range 100 kHz~30 MHz (AC-current up to 20 mA.). The so-called cable compensation function of the measuring facility allowed to eliminate the errors introduced by 1 m long cables and to keep constant the level (auto level function) of the sinusoidal current. Four gold tip contacts were pressed by springs to the sample surface. The errors introduced by the sample-holder were determined from the impedance vs. frequency characteristics of a thin copper short-circuiting plate. A computer controlled setup enables to measure precisely the magneto-impedance hysteresis loop [$Z(H)$] in an axial

static magnetic field of its intensity up to 12 kA/m.

3. Results and Discussion

The magnetization characteristics $M(H)$ of the stress relaxed sample and the samples annealed under various tensile stresses exhibit relatively small hysteresis. The stress-annealed samples display a typical hard-axis dependence of magnetization. The transverse anisotropy constant calculated for example for the sample annealed under maximum stress of 410 MPa (S6-sample) gave $K_u \approx 120$ J/m^3. This anisotropy manifests itself in the domain pattern (seen on the sample surface by magneto-optical Kerr effect setup) consisting of narrow strips directed perpendicularly to the ribbon axis.

The dependencies of the real, (R), and imaginary, (X), components of the impedance, Z, on external axial DC-field for the S1-sample (as-quenched) are shown in Fig. 1a and b. The obtained two-peak characteristics, were measured at various frequencies of the AC-current of 10 mA. These dependencies measured at 1 and 20 mA are almost identical so the influence of current intensity (in range of 1~20 mA) is practically negligible. A huge increase with the frequency of the stable contribution to the reactance X occurs because of the "external" (geometrical) inductance of the sample. The contribution of this inductance (not important from the point of view of physics) is canceled if the used system is calibrated (as is frequently the case) subtracting the impedance of the saturated sample. However, this contribution should be taken into account if the goal of the studies is of a practical nature.

The temperature dependence of the impedance in the range from room temperature up to 100 °C is not strong. For example, the maximum of impedance (Z_{max}) changes of about 1% for the S1-sample at 10 MHz.

Thermal treatment changes mainly the central region of the magneto-impedance characteristics, in particular the range between two maxima. The fact that all the characteristics measured in this studies display two maxima indicates that small local anisotropies are present even in the stress relaxed samples (S2, S3). However, in the latter samples the "inner region" (between the two maxima) is more narrow and shallow and the value of the maximum is larger than in those marked S1 and S4-S6.

Typical result of stress annealing on the $Z(H)$ characteristics is seen in Fig. 2, where the R-component dependencies on the DC-field for the S6-sample (at various

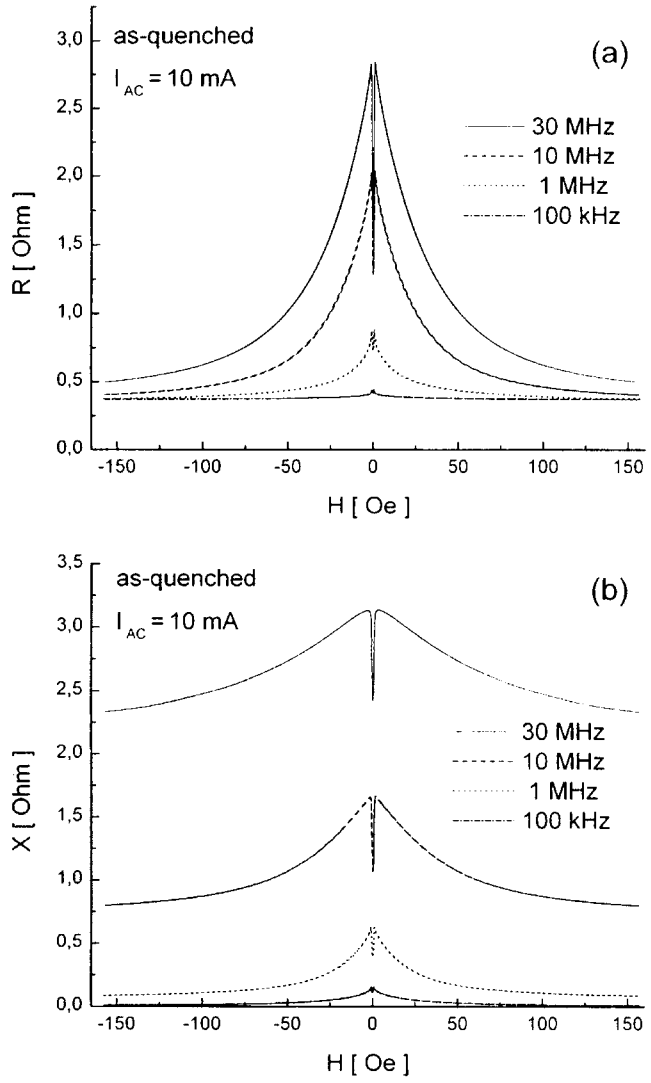

Fig. 1. Field dependence of real (a) and imaginary (b) components of impedance for S1-sample.

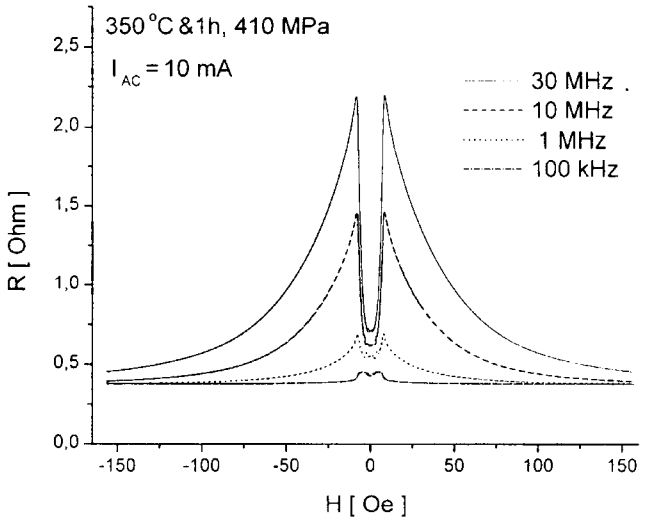

Fig. 2. Real (R) components of impedance vs. DC-field for stress annealed sample (S6).

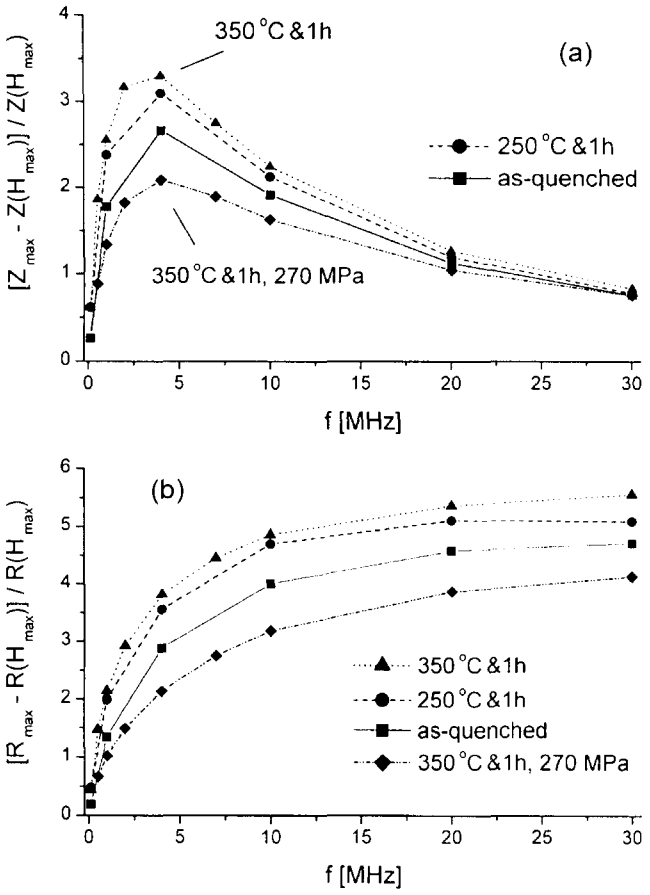

Fig. 3. Frequency dependence of magneto-impedance ratio (a) and MI ratio for R-component (b) for several samples.

frequencies of the AC-current) are presented. The most characteristic effect of thermal treatment under stress is that the "inner region" becomes wider and deeper and also the values of Z_{max} are lower. The shift of the maximum in $Z(H)$ characteristic (from H=0) corresponds with the estimated anisotropy field.

Fig. 3a shows the frequency dependence of the magneto-impedance ratio (defined as: $MI = [Z_{max}-Z(H_{max})]/ Z(H_{max}) \times 100\%$, where H_{max} is the maximum applied axial DC-field) for several of the studied samples. It is seen that for all of them, the MI ratio displays a maximum at about 4 MHz. The largest value of the MI (about 330%) is achieved for the stress relaxed sample (S3: 350 °C/1 h).

Similar ratio can be calculated for the R-component only: $(MI)_R = [R_{max}-R(H_{max})]/R(H_{max})$. Its frequency dependence is presented in Fig. 3b (for the same samples as those in Fig. 3a). This ratio increases monotonically with frequency, achieving 550% for the S3-sample at 30 MHz. Different behavior of the $(MI)_R$ ratio compared with that of MI is mainly due to the external inductance which affects strongly the reactance component. Thus, detection

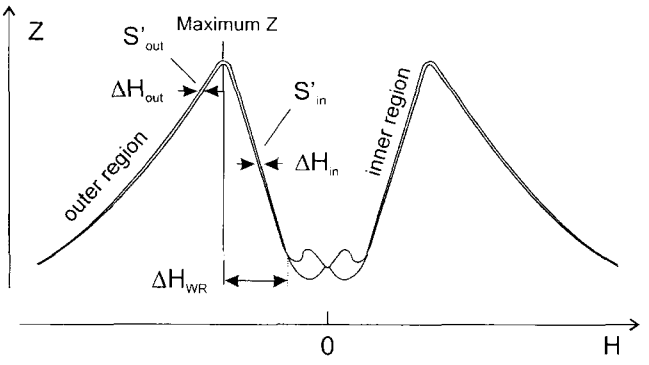

Fig. 4. Parameters of the $Z(H)$ hysteresis loop.

of only the R-component allows to achieve higher sensitivity and to use the range of higher frequencies (with no loss in sensitivity) in sensor application.

The MI-ratio gives information only about the magnitude of changes of Z. Therefore, the sensitivity parameter is usually introduced, e.g. in a form: $S = 2 \times MI/\Delta H_{1/2}$, where $\Delta H_{1/2}$ is the half-width of the $Z(H)$ curve (in the case of only one maximum). This formula gives, however

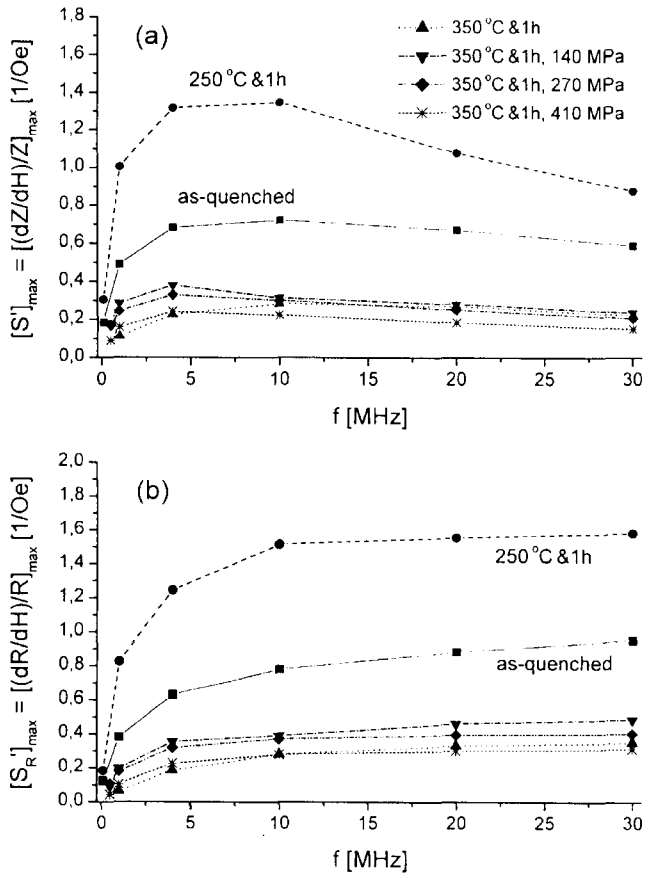

Fig. 5. Maximum sensitivity in the "inner region" vs. frequency (a) and R-component sensitivity (b) for several samples.

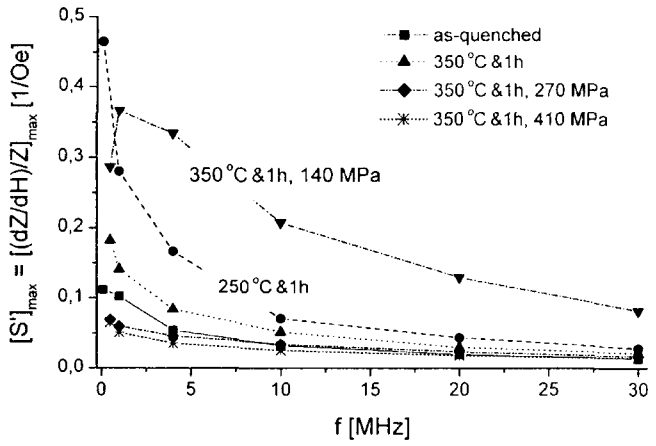

Fig. 6. Maximum sensitivity in the "outer region" vs. frequency for several samples.

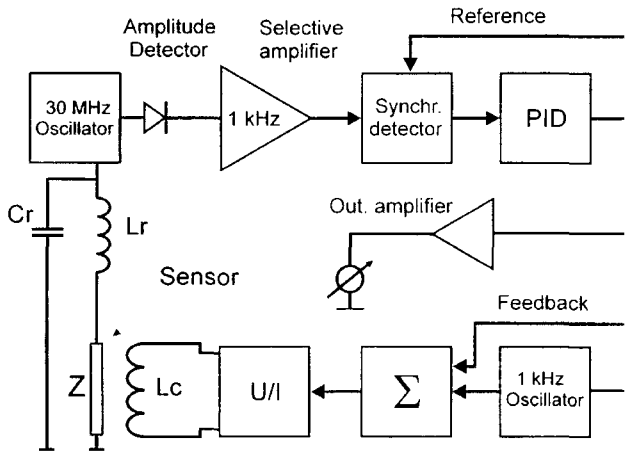

Fig. 7. Electronic circuit of designed magnetic field sensor.

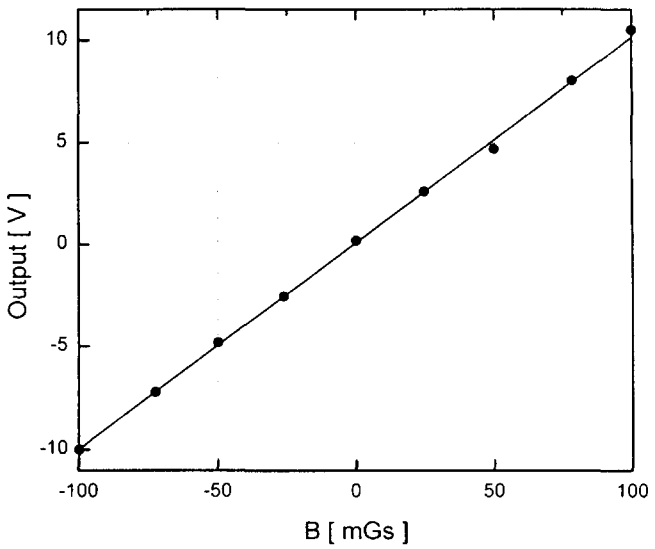

Fig. 8. Measured characteristic of the magnetic field sensor.

only a rough estimation of the sensitivity. In order to find an optimum working point, the sensitivity should be calculated locally. In this work a derivative is used to calculate the sensitivity: $S' = (dZ/dH)/Z$ and its maximum is determined separately in the inner and outer regions (see Fig. 4). The plots of $[S']_{max}$ vs. frequency calculated for the impedance modulus in the inner region are shown in Fig. 5a. For the heat treated samples $[S']_{max}$ is lower than for the S1-sample (as-quenched), except the S2-sample (250 °C/1 h) for which sensitivity is much higher ($[S']_{max} \approx 135\%$/Oe at 10 MHz). The same concerns the maximum of sensitivity calculated for the *R*-component and defined as $[S_R']_{max} = [(dR/dH)/R)]_{max}$ with an exception that the presented in Fig. 5b dependencies display no maximums. The S_R' sensitivity is higher than that for the impedance (e.g. $[S_R']_{max} \approx 160\%$/Oe at 30 MHz for S2). Within the outer region the sensitivities $[S']_{max}$ and $[S_R']_{max}$ are much lower and their decrease with the frequency is generally faster as it is seen in Fig. 6 showing $[S']_{max}$ vs. frequency.

The $Z(H)$ hysteresis for the inner and outer region obtained at different frequencies has been compared. The hysteretic shifts of the $Z(H)$ curve were determined at the points of maximum sensitivity (see Fig. 5). The hysteresis of the impedance (not large) is generally smaller in the inner region, e.g. less than 0.1 Oe for the S2-sample (for S3 below 0.02 Oe).

Because of specific shape of the $Z(H)$ curve an additional parameter, DH_{WR}, ("working range") can be introduced for the inner region. This parameter can be roughly estimated calculating the difference between the field of maximum Z and the field at which the hysteretic behavior of $Z(H)$ rapidly increase (see Fig. 4). The samples with intentionally induced magnetic anisotropy have generally smaller magneto- impedance ratio and sensitivity, however, they show wider working range (e.g. $\Delta H_{WR} \approx 6$ Oe for the S6 sample compared with $\Delta H_{WR} < 1$ Oe for S1).

The studied material has been utilized to design magnetic field sensor (Fig. 7). In this unique construction a straight 25 mm long piece of amorphous ribbon is a part of the parallel resonant circuit (L_r, C_r). The impedance of the sensor determines the quality factor of the circuit and, therefore the amplitude of oscillation of the free-running oscillator. The sensing element is connected in series with the inductance (L_r), so the changes of its own inductance are less important than changes of the AC-resistance. Magnetic field modulation and the feedback circuit are used to obtain the linear response of the device (see Fig. 8). The modulation and feedback current (AC+DC) is fed to the coil (L_c) wound around the sensor. The sensor

operates at zero average magnetic fields (external field minus compensation field). The sensitivity of the prototype is limited by the output noise to 500 μGs (5×10^{-8} T) for the unshielded sensor.

Depending on the given solution, the shape of the sensing element (ribbon) can be changed. Ring-like shape can be used for contact-less DC current measurement (DC-current conductor placed along the axis of ring) with the sensitivity of the order of 1 mA and a separation enough for high voltage isolation.

Acknowledgements

This study was performed within the project No. 8 T11B 049 19 granted by the State Committee for Scientific Research (Poland). This work was also partially supported by KOSEF (Korea Science and Engineering Foundation) and by European Community Program ICA1-CT-2000-70018 (Center of Excellence CELDIS in the Institute of Physics, Polish Acad. Sci.).

References

[1] M. Vázquezm, J. Magn. Magn. Mater. **226-230**, 693 (2001).
[2] Beach, R. S. and Berkowitz, A. E. Appl. Phys. Lett. **64**, 3652 (1994).
[3] Panina, L. V. and Mohri, K. Appl. Phys. Lett. **65**, 1189 (1994).